2012

Experimental Investigation on Evaporation Heat Transfer and Pressure Drop Characteristics of HFC-161 in a Horizontal Smooth Tube

Peng Li
21027134@zju.edu.cn

Xue Hui Wang

Xiaohong Han

Guangming Chen

Experimental Investigation on Evaporation Heat Transfer and Pressure Drop Characteristics of HFC-161 in a Horizontal Smooth Tube

Peng LI, Xue Hui WANG, Xiao Hong HAN* and Guang Ming CHEN

Institute of Refrigeration and Cryogenics, Zhejiang University, Hangzhou, China, 310027

* Corresponding Author. Tel.:+86-571-87953196; fax:+86-571-87953196
E-mail address: hanxh66@zju.edu.cn

ABSTRACT

The evaporation heat transfer and pressure drop characteristics of HFC-161 in a horizontal smooth tube with an inside diameter of 9 mm was experimentally investigated. The local heat transfer coefficient and total pressure drop were measured at the heat flux ranging from 15 – 25 kW/m^2, the mass flux ranging from 100 – 200 kg/(m^2 s), and the evaporation temperature of 5, 10 ℃. The experimental results showed that the evaporation heat transfer coefficient increased with the vapor quality except in the high vapor quality region, increased with the mass flux and the heat flux, and decreased with the saturation temperature across the experimental conditions. By comparison, the measured heat transfer coefficient of HFC-161 is higher than that of R22. In addition, the measured total pressure drop of two-phase HFC-161 in the test tube increased strongly with the mass flux within the experimental range. The presented results are helpful in designing more compact and effective heat transfer exchangers for the air-conditioning systems using HFC-161.

1. INTRODUCTION

Energy shortage and environmental pollution have been the important factors of restricting and influencing the sustainable development of humanity. In the air conditioning field, the study of alternative refrigerants is recognized as one of the urgent issues to ease ozone depletion and global warming. For the excellent environmental performance (ODP = 0, GWP = 12), high energy efficiency and good commonality with the existing systems (Xuan and Chen, 2005), HFC-161 is another promising alternative refrigerant. So far, a lot of researches about HFC-161 and the related refrigerant mixtures have been conducted on the PVTx (Chen *et al.*, 2005), the saturated vapor pressure (Chen *et al.*, 2005), the vapor-liquid equilibrium (Han *et al.*, 2006, 2010), the solubility with POE (Han *et al.*, 2010), cycle performance (Han *et al.*, 2007), etc. By these studies, abundant experimental data has been acquired and the application process of HFC-161 is promoted. However research for the evaporation heat transfer and pressure drop characteristics of HFC-161 and its mixtures has not been found in open literatures. When a new refrigerant is proposed, the heat transfer and pressure drop characteristics is usually regarded as one of the research focuses, which is necessary for analyzing performance of the heat exchangers and the actual air conditioning systems. Hsieh *et al*. (2007) experimentally studied the saturated flow boiling heat transfer of refrigerant R-410A in a horizontal annular finned duct, the results showed that the boiling curves are mainly affected by the imposed heat flux and refrigerant mass flux. Greco and Vanoli (2005) measured the flow boiling heat transfer coefficients of R22, R134a, R507, R404A and R410A inside a smooth horizontal tube (6 mm I.D., 6 m length), the results showed that the heat transfer coefficients of R134a were higher than that of all the other refrigerant fluids. Lee *et al.* (2005) presented the experimental results of heat transfer characteristic and pressure gradients of hydrocarbon refrigerants R-290, R-600a, R-1270 and HCFC refrigerant R-22 during evaporating inside horizontal double pipe heat exchangers, the obtained heat transfer coefficient had coincided with most of the Kandlikar's correlation. Hu *et al.* (2010) experimentally investigated the two-phase heat transfer characteristics of R410A–POE oil mixture and R22-mineral oil mixture flow boiling inside a horizontal C-shape curved smooth tube, the test results showed that the

curvature of C-shape curved smooth tube deteriorates the flow boiling heat transfer. In order to enrich the database of the potential alternative refrigerant and supply reference for designing more compact and effective evaporators of air conditioning using HFC-161, the evaporation heat transfer and pressure drop characteristics of HFC-161 in a horizontal smooth tube with an inside diameter of 9 mm were investigated by experimental methods. Moreover, in order to reflect the heat transfer performance of the promising candidate refrigerant HFC-161, the measured result was compared with that of R22.

2. EXPERIMENTAL APPARATUS AND PROCEDURE

2.1 Test Facility

The experimental apparatus used to measure the evaporation heat transfer coefficient and pressure drop of HFC-161 is schematically given in Figure 1. It consists of a DC power supply, a data acquisition system and three main loops: the test refrigerant loop, the cooling loop with a secondary vapor compression system, and the pre-heating loop with a thermostatic water tank. The test loop includes a test tube (horizontal smooth tube, 9 mm I.D., 4 m length), two sight glasses, a condenser, a receiver, a gear pump (variable-speed), an accumulator, a filter/dryer, a Coriolis mass flow meter (CMF) and a pre-evaporator. During the experiment, the refrigerant with a certain vapor quality from the pre-evaporator enters the test section and evaporates when heated by the DC power supply; then the boiling refrigerant with a higher vapor quality flows into the condenser and will be condensed by the low temperature water–glycol (cooled by the vapor compression system) and; then the sub-cooled refrigerant in the receiver will be driven by the gear pump through the CMF into the pre-evaporator. The pressure of the refrigerant loop was controlled by adjusting the temperature and flow rate of the water-glycol in the condenser. The flow rate of HFC-161 was controlled by adjusting the input frequency of the magnetic gear pump. The imposed heat flux to evaporate the refrigerant was controlled by adjusting the electrical current from the DC power supply. The inlet vapor quality of HFC-161 was controlled by adjusting the amount of heat supplied to the refrigerant in the pre-evaporator.

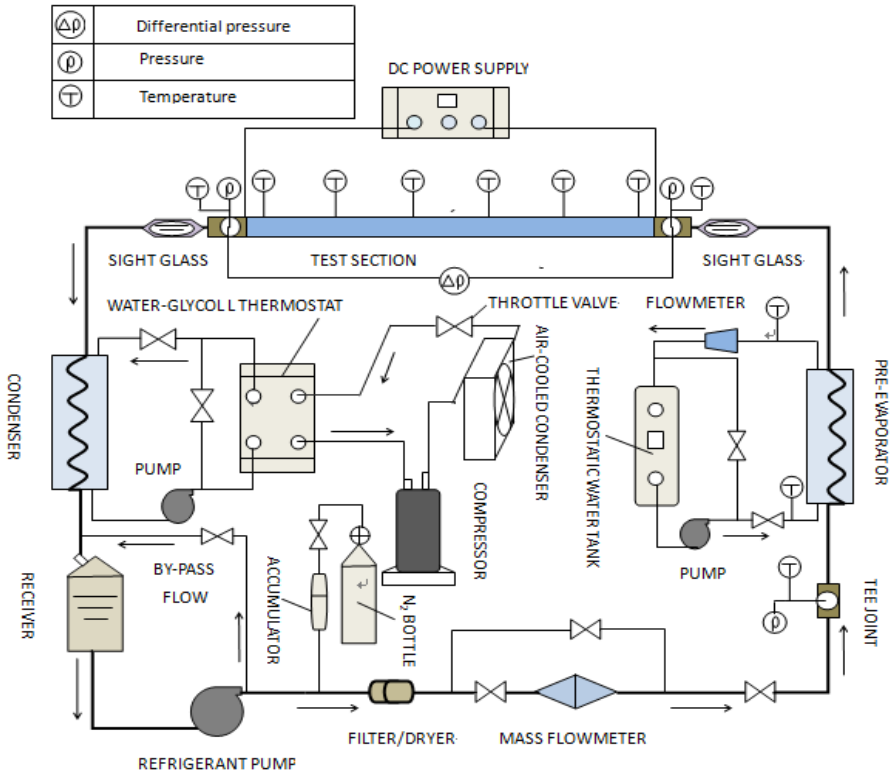

Figure 1: Schematic diagram of the experimental system

The test section is shown in Figure 2. The test tube (copper tube) has an inside diameter of 9 mm and an outside diameter of 12 mm. It is heated by a DC power supply through the silicone rubber heating band glued on the outer surface of the pipe. A thin layer of heat conduct silicone is used to boost and spread the heat transferred to the refrigerant. The local temperature of outer surface of the test tube was measured using T - type thermocouples with an accuracy of ±0.1 ℃ mounted in six stations along the axial direction (seen in Figure 2), and each station had four thermocouples clamped on the top, bottom, left, right sides, respectively. Two four-wire Pt100 resistance thermometers with an accuracy of ±0.03 ℃ and two pressure transducers with an accuracy of ±0.2 % F.S were inserted in the refrigerant flow stream at the inlet and the outlet of the test section, respectively. In addition, a differential pressure transducer with an accuracy of ±0.1 % F.S. was used to measure the total pressure drop. All the measured parameters were logged by a data acquisition.

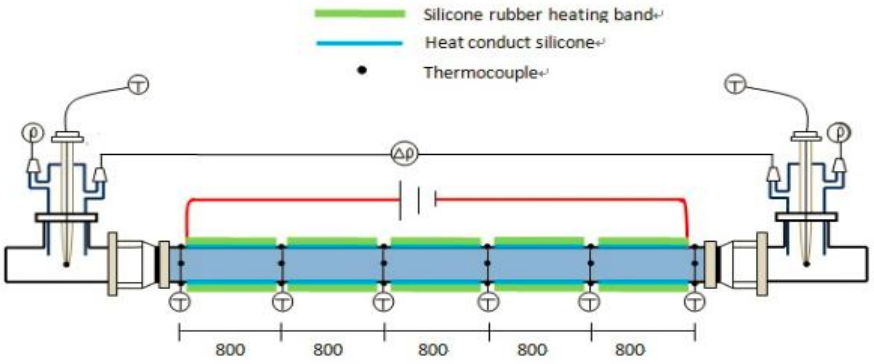

Figure 2: Schematic diagram of the test section

2.2 Experimental Conditions

The experimental conditions in this work are given in Table 1 and the following figures present the variations of heat transfer coefficient with these conditions.

Table 1: Experimental conditions

Refrigerant	Saturation temperature (℃)	Mass flux (kg/m^2 • s)	Heat flux (kW/m^2)	Inlet vapor quality
HFC-161	5, 10	100 – 200	15 – 25	0.1 – 1

2.3 Data Reduction

The local heat transfer coefficient, at each downstream location, is defined in Equation (1):

$$q = \frac{Q}{A} = \frac{Q}{\pi \cdot D_i \cdot L} = h_{\text{ev}} \left(T_{\text{wi}} - T_{\text{sat}}\right) \quad (1)$$

where q is the heat flux, h_{ev} is the evaporation heat transfer coefficient, T_{wi} is the inside wall temperature, and T_{sat} is the measured evaporation temperature. Thanks to the accurate test section insulation, the heat losses are negligible and it is possible to calculate the heat flux when the total heat input (that is measured considering the values of the voltage and of the current, $Q = U \cdot I$) is known.

The inside wall temperature of the test section, T_{wi}, is estimated from the measured outside wall temperature T_{wo} (seen in Equation (2)), by applying the one-dimensional, radial, steady-state heat conduction equation:

$$T_{wi} = T_{wo} - \frac{Q \cdot \ln \frac{D_o}{D_i}}{2 \cdot \pi \cdot \lambda_w \cdot L} \quad (2)$$

where λ_w and L are the thermal conductivity and the length of the test tube, respectively. T_{wo} is the average temperature of the one at the top, two at the side and one at the bottom of the outside surface, seen in Equation (3):

$$T_{wo} = \frac{T_{wo,top} + 2 \cdot T_{wo,side} + T_{wo,bottom}}{4} \quad (3)$$

The local vapor quality is determined by Equation (4):

$$x = \frac{i - i_L}{i_{LG}} \quad (4)$$

where i_L is the specific enthalpy of the saturated liquid at the measured pressure, i_{LG} is the latent heat of vaporization, i is determined by Equation (5):

$$i = i_{in} + \frac{qA}{G} \quad (5)$$

where i_{in} is the refrigerant specific enthalpy at the inlet of the test section, which is calculated from the sub-cooled liquid by an energy balance in the pre-evaporator. G is the actual refrigerant mass flux, q is the actual heat flux and A is the local area of the tube.

3. RESULTS AND DISCUSSION

3.1 Evaporation Heat Transfer Coefficient

The present experiments are conducted for the refrigerant mass flux ranging from 100 to 200 kg/(m^2 s), the imposed heat flux from 15 to 25 kW/m^2 , and the refrigerant saturation temperature of 5, 10 ℃.

The variations of the measured heat transfer coefficients with the vapor quality at three different mass fluxes (100, 150, 200 kg/(m^2 s) and two different saturation temperatures (5, 10 ℃) for q = 15 and 25 kW/m^2 are shown in Figures 3 ~ 4, respectively.

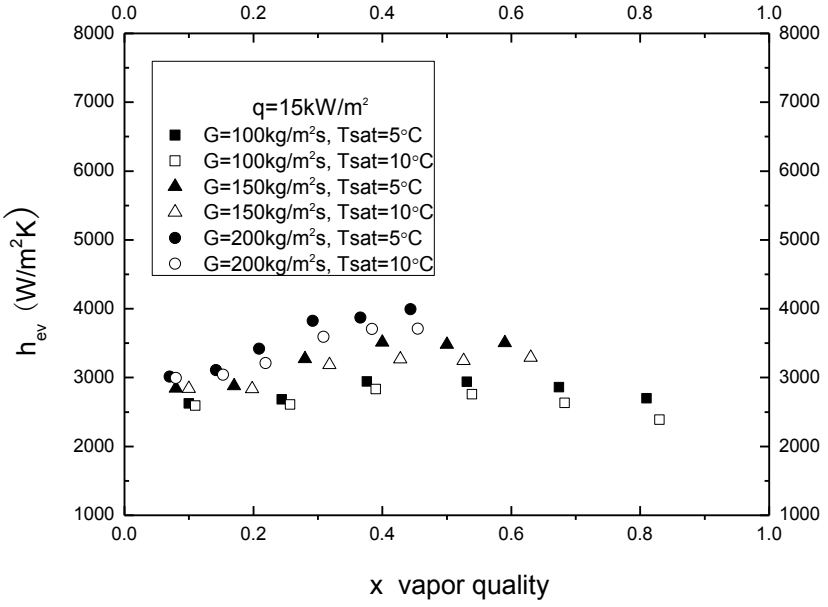

Figure 3: Local heat transfer coefficient versus vapor quality for various mass fluxes and saturation temperatures, at q = 15 kW/m^2

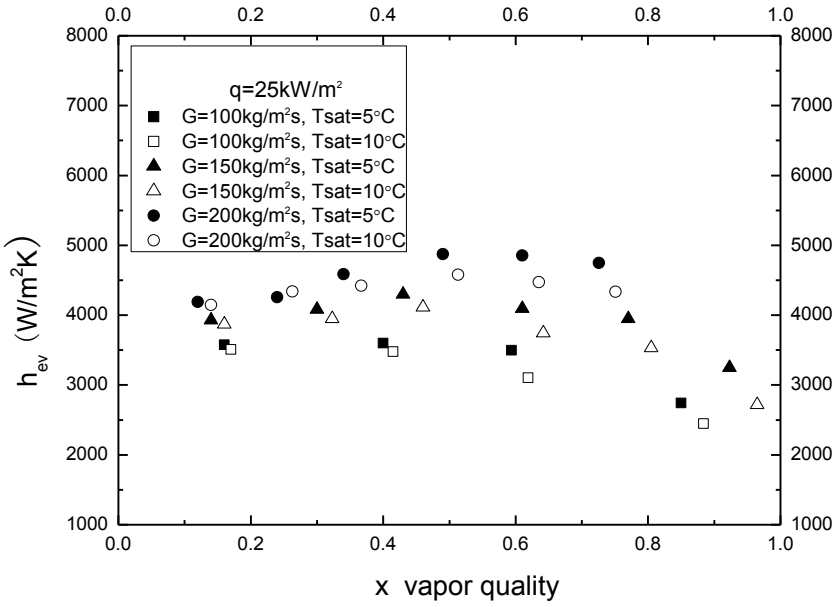

Figure 4: Local heat transfer coefficient versus vapor quality for various mass fluxes and saturation temperatures, at q = 25 kW/m^2

The results from Figures 3 ~ 4 indicate that the local heat transfer coefficients increase with the vapor quality until the vapor quality increases to a certain value (about 0.5 – 0.6). And further observation from Figures 3 ~ 4 reveals that at a higher heat flux or a smaller mass flux, the inflection point of the heat transfer coefficients corresponds to a smaller vapor quality. It also can be seen in Figures 3 ~ 4 that at given heat flux q and saturation temperature *Tsat*, the evaporation heat transfer coefficients increase with the mass flux. And, the difference of heat transfer coefficients among different mass fluxes increases with increasing vapor quality. For example, when the heat flux and saturation temperature are fixed at 15 kW/m^2 and 5 ℃, respectively, the heat transfer coefficient at G = 150 kg/ (m^2 · s) is about 5 % – 20 % higher than that at G = 100 kg/ (m^2 · s) and heat transfer coefficient at G = 200 kg/ (m^2 · s) is about 5 % – 10 % higher than that at G = 150 kg/ (m^2 · s) among the lower vapor quality region (0.1 < x < 0.4). Whereas, the corresponding heat transfer coefficient increase percentages among the higher vapor quality region (x > 0.4) are about 20 % – 25% and 10 % – 15 %, respectively.

The variations of the measured heat transfer coefficients with the vapor quality at three different heat fluxes (15, 20, 25 kW/m^2) and two different saturation temperatures (5, 10 ℃) for G = 100 and 200 kg/(m^2 s) are shown in Figures 5 ~ 6, respectively.The results from Figures 5 ~ 6 indicate that at given mass flux G and saturation temperature T_{sat}, the evaporation heat transfer coefficients increase with the heat flux. But the difference of heat transfer coefficient among different heat fluxes reduces with increasing vapor quality. For example, when the mass flux and saturation temperature are fixed at 100 kg/ (m^2 s) and 5 ℃, respectively, the heat transfer coefficient at q = 20 kW/m^2 is about 10 % – 20 % higher than that at q = 15 kW/m^2 and heat transfer coefficient at q = 25 kW/m^2 is about 10 % - 15 % higher than that at q = 20 kW/m^2 among the lower vapor quality region (0.1 < x < 0.4). Whereas, the corresponding heat transfer coefficient increase percentages among the higher vapor quality region (0.4 < x < 0.8) are about 5 % – 10 % and 2 % – 10 %, respectively. Even when the vapor quality exceeds 0.8, the heat transfer coefficient at a higher heat flux is lower than that at a lower heat flux.

On the other hand, the variations of the evaporation heat transfer coefficient with the saturation temperature of the refrigerant can be also obtained from Figures 3 ~ 6. There is a decrease in the heat transfer coefficient with the increasing saturation temperature across the experimental vapor quality region at fixed mass flux and heat flux. But the decrease is not very obvious, heat transfer coefficient at the evaporation temperature of 5 ℃ is about 5 % higher than that at 10 ℃. This may be attributed to the fact that the refrigerant latent heat of vaporization as well as the liquid viscosity slowly decline with the increase of temperature.

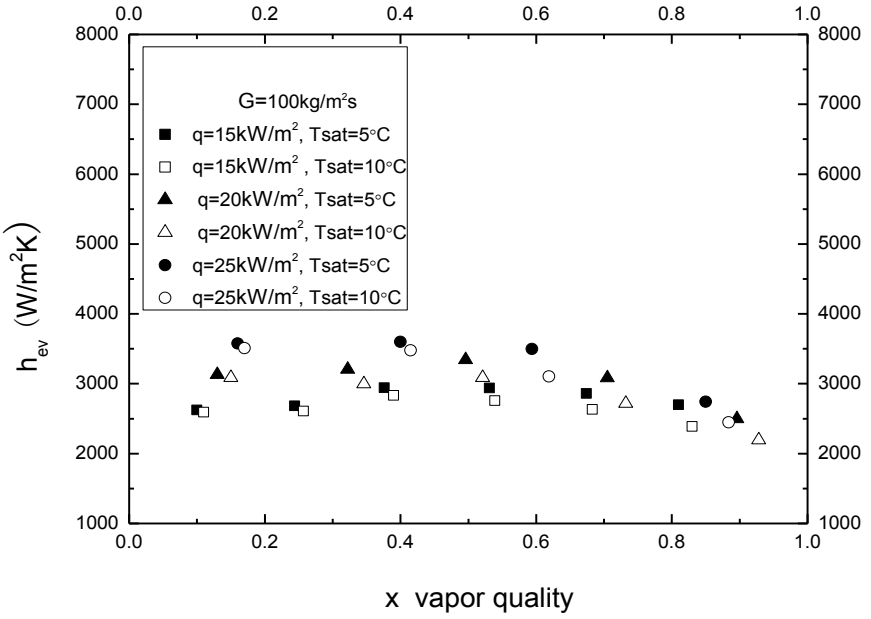

Figure 5: Local heat transfer coefficient versus vapor quality for various heat fluxes and saturation temperatures, at G = 100 kg/(m^2 • s)

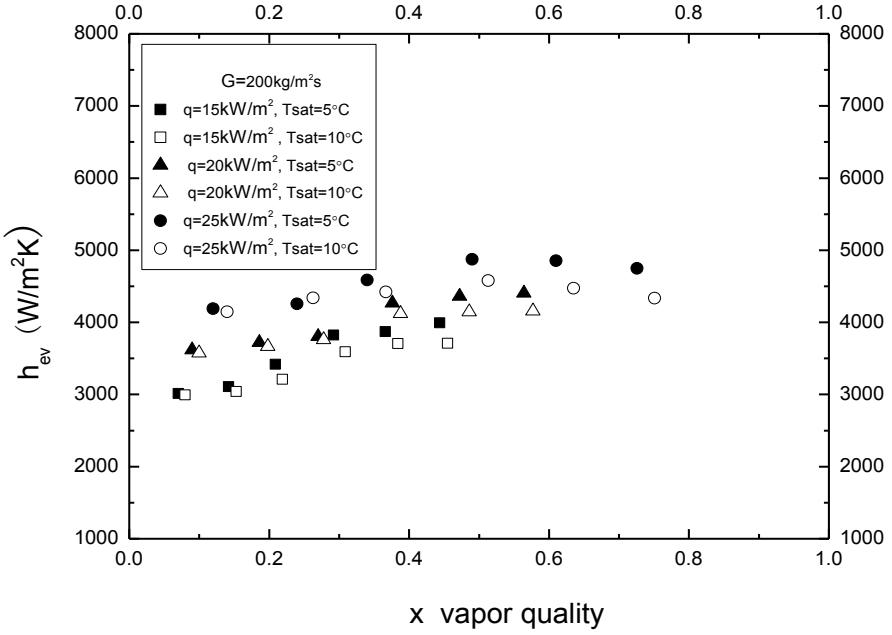

Figure 6: Local heat transfer coefficient versus vapor quality for various heat fluxes and saturation temperatures, at G = 200 kg/(m^2 s)

3.2 Pressure Drop

The pressure drop of HFC-161 flow boiling along the test tube is measured directly by the differential pressure transducer installed between the inlet and outlet of the test tube.

Figure 7 presents the variation of the total pressure drop of HFC-161 flowing along the test tube with the mass flux for various heat fluxes and saturation temperatures. The results indicate that the total pressure drop increases strongly with the mass flux within the experimental range. For example, when the heat flux and saturation temperature are fixed at 15 kW/m^2 and 5 ℃, respectively , pressure drop at G = 200 kg/(m^2 · s) is about 50 % higher than that at G =150 kg/(m^2 · s) and pressure drop at G = 150 kg/(m^2 · s) is about 80 % higher than that at G = 100 kg/(m^2 s), respectively. In addition, Figure 7 also shows that the pressure drop decreases with the increase of saturation temperature, pressure drop at *Tsat* = 5 ℃ is about 10 % higher than that at *Tsat* = 10 ℃. This may be attributed to the fact that as the saturation temperature increases, the refrigerant viscosity decrease, which will lead to the decrease of the pressure drop. Finally, it can be seen from Figure 9 that the difference of pressure drop between different heat fluxes is slight. Therefore, influence of heat flux on the pressure drop may be negligible.

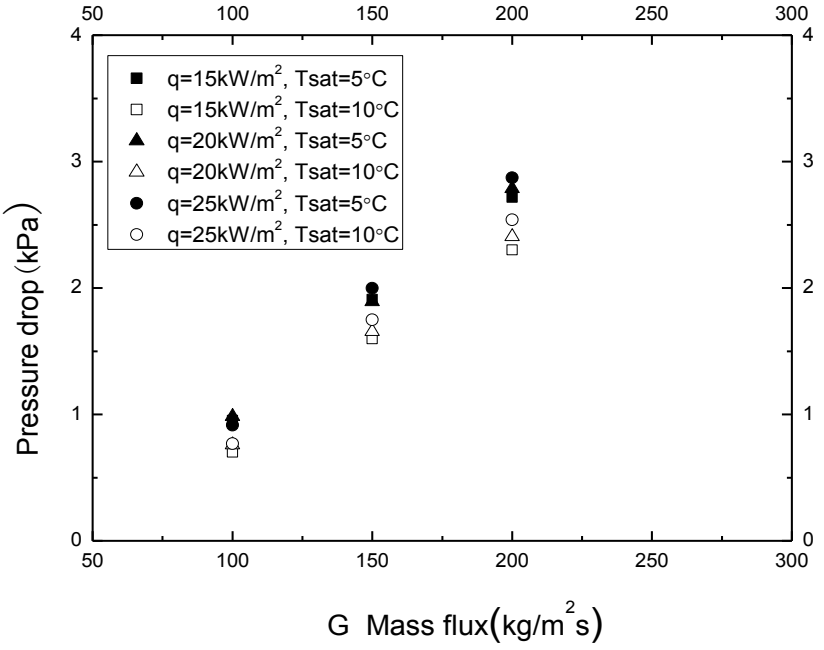

Figure 7: Pressure drop versus mass flux for various heat fluxes and saturation temperatures

3.3 Comparison between HFC-161 and R22

To analyze the heat transfer performance of the promising candidate of R22, Figure 8 shows a comparison between the evaporation heat transfer coefficient of HFC-161 and R22, at q = 10 kW/m^2 and *Tsat* = 5 ℃. It can be seen in Figure 8 that for any mass flux, the evaporation heat transfer coefficient of HFC-161 is higher than that of R22, especially in the high vapor quality region. When the vapor quality exceeds 0.4, heat transfer coefficient of HFC-161 is about 10 % – 25 % higher than that of R22. The enhance of heat transfer performance may lie in the difference in the thermodynamic properties of the two refrigerants. For example, the vaporization latent heat of HFC-161 is about 84 % higher than that of R22 at *Tsat* = 5 ℃.

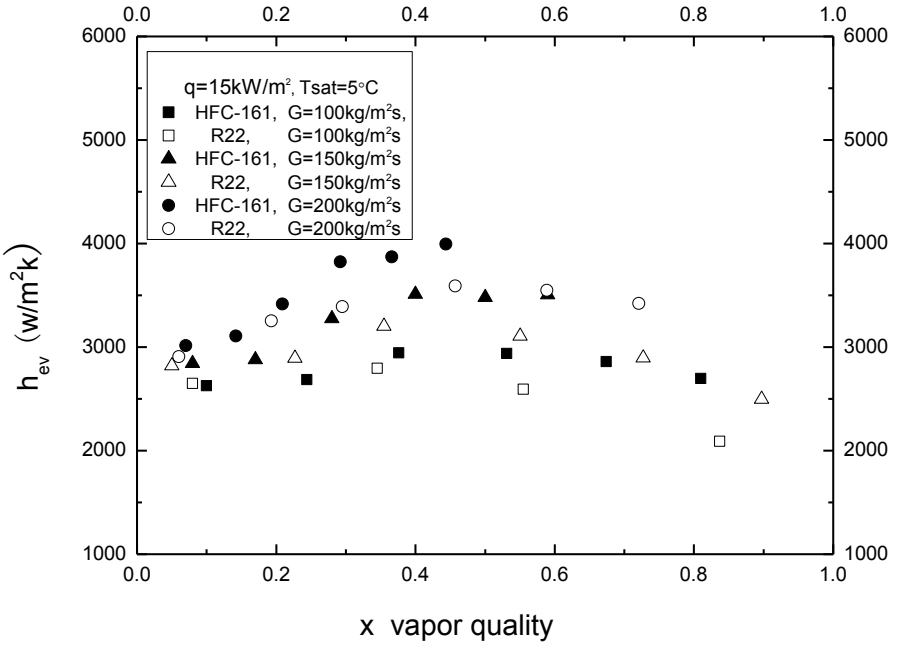

Figure 8: Comparison of heat transfer coefficients between HFC-161 and R22 for various mass fluxes, at q = 15 kW/m^2, *Tsat* = 5 ℃

4. CONCLUSIONS

HFC-161 is regarded as another promising alternative refrigerant of R22. The evaporation heat transfer and pressure drop characteristics of HFC-161 in a horizontal smooth tube with an inside diameter of 9 mm was experimentally investigated. The local heat transfer coefficients were measured at the heat flux ranging from 15 – 25 kW/m^2, the mass flux ranging from 100 – 200 kg/(m^2 s), and the evaporation temperature of 5 ℃, 10 ℃. The results are summarized as follows:

- The local heat transfer coefficients increase with the vapor quality until the vapor quality increases to a certain value (about 0.5 – 0.6).
- The evaporation heat transfer coefficients of HFC-161 increase with the mass flux and the heat flux; the difference of heat transfer coefficient among different mass fluxes increases with increasing vapor quality, and the difference of heat transfer coefficient among different heat fluxes reduces with increasing vapor quality.
- There is a decrease in the evaporation heat transfer coefficient with the increasing saturation temperature across the experimental conditions.
- The total pressure drop increases strongly with the mass flux within the experimental range.
- The evaporation heat transfer coefficient of HFC-161 is higher than that of R22, especially in the high vapor quality region.

NOMENCLATURE

h_{ev}	evaporation heat transfer coefficient	(W/(m^{2}K))	q	heat flux	(kW/m^2)
T_{wi}	inside wall temperature	(℃)	T_{wo}	outside wall temperature	(℃)
Q	total heat input	(W)	U	voltage	(V)
I	current	(A)	A	heat transfer are	(m^2)
L	length of the test tube	(m)	Di	inside diameter	(m)
Do	outside diameter	(m)	G	mass flux	(kg/(m^2 s))
T_{sat}	saturation temperature	(℃)	x	vapor quality	(-)
i	enthalpy	(kJ/kg)	λ_w	thermal conductivity	(W/(m k))

REFERENCES

Chen, Q., Chen, G.M., Hong, R.H., 2005, Vapor pressure measurements of ethyl fluoride, *J. Chem. Eng. Data,* vol.50, no. 5: p. 1586-1588.

Chen, Q., Hong, R.H., Chen, G.M., 2005, Gaseous PVT properties of ethyl fluoride, *Fluid Phase Equilib.*, vol. 237, no. 1-2: p. 116-119.

Greco, A., Vanoli, G.P., 2005, Flow-boiling of R22, R134a, R507, R404A and R410A inside a smooth horizontal tube, *Int. J. Refrig.*, vol.28, no.6: p. 872-880.

Han, X.H., Chen, G.M., Li, C.S., Qiao, X.G., Cui, X.L., 2006, Isothermal vapor-liquid equilibrium data for the binary mixture refrigerant pentafluoroethane (R125) + fluoroethane(R161) at 265.15, 275.15, 283.15, 293.15, 303.15 and 303.15K with a recirculating still, *J. Chem. Eng. Data*, vol. 51, no. 4: p. 1232-1235.

Han, X.H., Gao, Z.J., Xu, Y.J., Qiu, Y., Ming, X.W., Wang, Q., Chen, G.M., 2010, Isothermal Vapor-liquid equilibrium data for the binary mixture difluoromethane(R-32)+ ethyl fluoride (R-161) over a temperature range from 253.15 to 303.15K , *Fluid Phase Equilib.*, vol. 299, no. 1: p.116-121.

Han, X.H., Wang, Q., Zhu, Z.W., Chen, G.M., 2007, Cycle performance study on R32/R125/R161 as an alternative refrigerant to R407C, *Appl. Therm. Eng.*, vol. 27, no.14-15: p. 2559-2565.

Han, X.H., Zhu, Z.W., Chen, F.S., Xu, Y.J., Gao, Z.J., Chen, G.M., 2010, Solubility and Miscibility for the Mixture of (Ethyl Fluoride + Polyol Ester Oil), *J. Chem. Eng. Data*, vol. 55, no. 9: p. 3200-3207.

Hsieh, Y.Y., Lie, Y.M., Lin, T.F., 2007, Saturated flow boiling heat transfer of refrigerant R-410A in a horizontal annular finned duct, *Int. J. Heat Mass Transfer*, vol. 50, no.7-8: p.1442–1454.

Hu, H.T., Ding, G.L., Wei, W.J., Huang, X.C., Wang, Z.C., 2010, Heat transfer characteristics of refrigerant-oil mixtures flow boiling in a horizontal C-shape curved smooth tube, *Int. J. Refrig.*, vol. 33, no.5: p. 932-943.

Lee, H.S., Yoon, J.I., Kim, J.D., Bansal, P., 2005, Evaporating heat transfer and pressure drop of hydrocarbon refrigerants in 9.52 and 12.70 mm smooth tube, *Int. J. Heat Mass Transfer*, vol. 48, no.6: p. 2351–2359.

Xuan, Y.M., Chen, G.M., 2005, Experimental study on HFC-161 mixture as an alternative refrigerant to R502, *Int. J. Refrig.*, vol. 28, no. 3: p. 436-441.

ACKNOWLEDGEMENTS

This work has been supported by the Nation Natural Science Foundation of China (Grant No. 50806063 and No. 51176166)